Human-Like Stable Bipedal Walking with a Large Stride by the Height Variation of the Center of Mass Using an Evolutionary Optimized Central Pattern Generator

Young-Dae Hong, Chang-Soo Park, and Jong-Hwan Kim

Abstract— **This paper proposes human-like stable bipedal walking with a large stride by the height variation of the center of mass (COM) using an evolutionary optimized central pattern generator (CPG). A modifiable walking pattern generator (MWPG) is utilized to generate a walking pattern for the bipedal robot. For the height variation of the COM, its height trajectory is generated by the CPG. A sensory feedback is utilized to compensate the disturbance caused by the height variation. Besides, the CPG is optimized by the quantum-inspired evolutionary algorithm (QEA) to obtain the desired output signals from the CPG. The proposed method is applied to a simulation model of the small-sized bipedal robot, HanSaRam-IX (HSR-IX), developed at the Robot Intelligence Technology laboratory, KAIST and the effectiveness is demonstrated through the simulations.**

I. INTRODUCTION

Recent researches have focused on the development of bipedal robots capable of stable walking [1]–[3] with the methods for walking pattern generation [4]–[7]. Particularly, the 3-D linear inverted pendulum model (3-D LIPM) [4] is the most widely utilized method to generate the walking pattern for the bipedal robot. Besides, based on the 3-D LIPM, various methods for walking pattern generation were developed [8]–[11]. In the 3-D LIPM, the height of the center of mass (COM) is set as a constant value. Thus, it is possible to decouple the sagittal and lateral COM motion equations. However, the constant COM height makes the bipedal robot walk unnaturally with a small stride. To overcome this problem, the COM height needs to be variable for a large stride like humans do by varying the hip height.

For this purpose, Kurazume *et al.* introduced knee stretch index and knee torque index for evaluating the efficiency of the use of the knee joints, and then the up-and-down COM motion was generated by optimizing these indexes [12]. Morisawa *et al.* presented a generation method of the COM motion constrained on the parametric surface which defines the relative COM height from the landing foot position [13]. Sekiguchi *et al.* developed a up-and-down COM motion generated by the vertical pivot motion of the 3-D LIPM [14]. Terada *et al.* presented an analytic solution to treat the vertical COM motion using a 3-D symmetrization method [15]. Shimmyo *et al.* utilized the virtual plane method based on the idea of a virtual zero moment point (ZMP) to generate the up-and-down COM motion [16], [17]. Li *et al.* proposed a hip pattern generator using the sinusoidal function and a feet pattern generator for heel-strike and toe-off motions [18].

This paper proposes human-like stable bipedal walking with a large stride by the height variation of the COM using an evolutionary optimized central pattern generator (CPG). The CPG is one of the biologically inspired approaches [19] and it generates rhythmic signals by using neural oscillators [20]. Using the CPG, there were approaches to generate the walking pattern for the bipedal robot [21]–[25]. In these approaches, by means of a sensory feedback in the CPG, the robot was able to walk stably maintaining the balance. However, it was unable to change the walking pattern in real-time. In this paper, a modifiable walking pattern generator (MWPG) [10], [11] is utilized to generate the walking pattern for the bipedal robot. It extended the conventional 3-D LIPM to allow the ZMP variation by the closed form functions. Namely, the MWPG enables the bipedal robot to change the walking pattern in real-time by the ZMP variation. For the height variation of the COM, its height trajectory is generated by the CPG. The sensory feedback is utilized to compensate the disturbance caused by the height variation. Besides, the CPG is optimized by the quantum-inspired evolutionary algorithm (QEA) [26], [27] to obtain the desired output signals from the CPG. The QEA is one of the evolutionary algorithms and it uses the concept of quantum computing. The proposed method is applied to a simulation model of the small-sized bipedal robot, HanSaRam-IX (HSR-IX), developed at the Robot Intelligence Technology laboratory, KAIST and the effectiveness is demonstrated through the simulations.

This paper is organized as follows. Section II presents the walking pattern generation by the MWPG. In Section III, the COM height variation is described. The CPG is reviewed and the COM height trajectory generation by the CPG is proposed with the sensory feedback. Also, the evolutionary optimization for the CPG is described with a brief introduction of the QEA. Section IV presents the simulation results and finally conclusions follow in Section V.

II. WALKING PATTERN GENERATION

In this paper, the MWPG [10], [11] is employed to generate the walking pattern for the bipedal robot and it is briefly summarized in the following. The bipedal walking is composed of single support phase and double support phase. In the single support phase, the primary dynamics

The authors are with the Department of Electrical Engineering, KAIST, 335 Gwahak-ro, Yuseong-gu, Daejeon 305-701, Republic of Korea (e-mail: {ydhong, cspark, johkim}@rit.kaist.ac.kr).

978-1-61284-972-0/11/$26.00 ©2011 IEEE

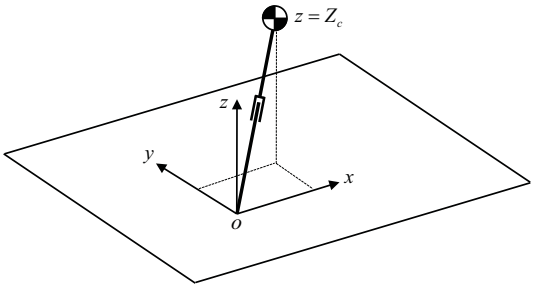

Fig. 1. Conventional 3-D LIPM.

of the bipedal robot is modeled as a 3-D LIPM as shown in Fig. 1 [4]. It is assumed that the support leg is a weightless telescopic limb and the mass of the robot is concentrated as a single point. In the conventional 3-D LIPM, the COM height variation is not considered. Namely, the COM height is constant Z_c. Consequently, it is possible to decouple the sagittal and lateral COM motion equations.

The dynamic equation of the 3-D LIPM for the angular momentum taken around the contact point between the pendulum model and ground surface is obtained by applying the Newton-Euler formulation as follows:

$$\mathbf{T}_{gr} + \mathbf{r}_{com} \times \mathbf{F}_{gr} = \frac{d}{dt}(\mathbf{r}_{com} \times \mathbf{L}) \tag{1}$$

where $\mathbf{T}_{gr} = [T_x \ T_y \ T_z]^T$ denotes the torque created by the ground reaction force (GRF), $\mathbf{r}_{com} = [x \ y \ z]^T$ is the vector from the contact point to the COM, $\mathbf{F}_{gr}$ and $\mathbf{L}$ denote the gravitational force and the linear momentum of the COM, respectively. From the assumption that the height of the COM, z is constant Z_c, (1) can be rewritten as follows:

$$\begin{bmatrix} \ddot{y} - \dfrac{g}{Z_c} y \\ \ddot{x} - \dfrac{g}{Z_c} x \end{bmatrix} = \begin{bmatrix} -\dfrac{T_x}{mZ_c} \\ \dfrac{T_y}{mZ_c} \end{bmatrix} \tag{2}$$

where m is the mass of the pendulum. The sum of the torques caused by the GRF is represented by the ZMP as follows:

$$\mathbf{T}_{gr} - \mathbf{r}_{zmp} \times \mathbf{F}_{gr} = \begin{bmatrix} 0 & 0 & M_z \end{bmatrix}^T \tag{3}$$

where $\mathbf{r}_{zmp} = [x_{zmp} \ y_{zmp} \ 0]^T$ denotes the ZMP and M_z is the yawing moment. From (3), T_x and T_y are obtained, and then by substituting them into (2), the dynamic equation of the 3-D LIPM can be rewritten as follows:

$$\begin{bmatrix} \ddot{y} - \dfrac{g}{Z_c} y \\ \ddot{x} - \dfrac{g}{Z_c} x \end{bmatrix} = -\frac{g}{Z_c} \begin{bmatrix} y_{zmp} \\ x_{zmp} \end{bmatrix}. \tag{4}$$

The above equation provides the relationship between the ZMP and the sagittal and lateral COM motions of the 3-D LIPM.

The solutions of (4), which mean the sagittal and lateral COM motions of the 3-D LIPM, are obtained by applying the inverse Laplace transform as follows:

Sagittal COM motion:

$$\begin{bmatrix} x_f \\ v_f T_c \end{bmatrix} = \begin{bmatrix} C_T & S_T \\ S_T & C_T \end{bmatrix} \begin{bmatrix} x_i \\ v_i T_c \end{bmatrix} - \frac{1}{T_c} \begin{bmatrix} \int_0^T S_T \bar{p}(t) dt \\ \int_0^T C_T \bar{p}(t) dt \end{bmatrix} \tag{5}$$

Lateral COM motion:

$$\begin{bmatrix} y_f \\ w_f T_c \end{bmatrix} = \begin{bmatrix} C_T & S_T \\ S_T & C_T \end{bmatrix} \begin{bmatrix} y_i \\ w_i T_c \end{bmatrix} - \frac{1}{T_c} \begin{bmatrix} \int_0^T S_T \bar{q}(t) dt \\ \int_0^T C_T \bar{q}(t) dt \end{bmatrix} \tag{6}$$

where $(x_i, v_i)/(x_f, v_f)$ and $(y_i, w_i)/(y_f, w_f)$ indicate initial/final COM position and velocity in sagittal and lateral planes, respectively. S_T and C_T are defined as $\sinh(T/T_c)$ and $\cosh(T/T_c)$, respectively, where $T_c = \sqrt{Z_c/g}$. T is the remaining single support time, and $p(t)$ and $q(t)$ are ZMP functions for the sagittal and lateral COM motions, respectively, where $\bar{p}(t) = p(T-t)$ and $\bar{q}(t) = q(T-t)$.

The first terms on the right-hand side of (5) and (6) represent homogeneous solutions of (4). The second terms represent particular solutions which allow more extensive sagittal and lateral COM motions by varying ZMP trajectories with $p(t)$ and $q(t)$. In the conventional 3-D LIPM, it is assumed that the ZMP is fixed at the contact point, thus the particular solutions have not been considered. Consequently, in the single support phase, the COM motion of the 3-D LIPM is predetermined and unmodifiable. Namely, it is impossible to independently modify the walking pattern, i.e. single and double support times, sagittal and lateral step lengths, and direction of the swing leg in the conventional 3-D LIPM. Whereas in the MWPG, the COM position and velocity can be changed independently at any time during the single support phase by the ZMP functions $p(t)$ and $q(t)$. It means that the MWPG enables the bipedal robot to change the walking pattern independently by the ZMP variation without any additional step for adjusting the COM motion. Moreover, since the closed form functions are used for the ZMP variation, the MWPG effectively reduces computational cost, which ensures a real-time calculation.

As an input of the MWPG, the command state (CS) is defined as follows [10], [11]:

Definition 1: Command state (CS) is defined as

$$\mathbf{c} \equiv [T_l^{ss} \quad T_l^{ds} \quad S_l \quad L_l \quad \theta_l \quad T_r^{ss} \quad T_r^{ds} \quad S_r \quad L_r \quad \theta_r]$$

where

$T_{l/r}^{ss}$: single support time during left/right support phase;
$T_{l/r}^{ds}$: double support time from left/right support phase to right/left support phase;
$S_{l/r}$: sagittal step length of left/right leg;
$L_{l/r}$: lateral step length of left/right leg;
$\theta_{l/r}$: direction of left/right leg.

The walking state (WS) of the 3-D LIPM, defined as the COM position and velocity, is derived for the CS [10], [11]. Then the COM trajectory satisfying the WS is obtained from

(5) and (6), and the trajectories of every joint of the bipedal robot are calculated by the inverse kinematics.

III. COM HEIGHT VARIATION

As mentioned in the previous section, the COM height of the 3-D LIPM is not variable in the conventional MWPG. In this paper, however, the COM height trajectory is generated by the evolutionary optimized CPG for human-like stable bipedal walking with a large stride.

A. Central Pattern Generator (CPG)

The CPG produces endogenously multi-dimensional rhythmic signals without a rhythmic sensory or central input. Also, the signals can be modified to deal with environmental perturbations using a sensory feedback. A neural oscillator for the CPG is used to generate the rhythmic signals and defined as follows [20]:

$$\begin{aligned} \tau \dot{u}_i &= -u_i - \sum_{j=1}^{n} w_{ij} y_j - \beta v_i + u_0 + feed_i \\ \tau' \dot{v}_i &= -v_i + y_i \\ y_i &= max(0, u_i) \end{aligned} \tag{7}$$

where u_i and v_i are the inner state and the self-inhibition state of the i-th neuron, respectively. u_0 is the external input signal which affects the output amplitude and y_i is the output signal. w_{ij} is the connecting weight which determines the phase difference between the i-th and j-th neurons, β is the weight of the self-inhibition, and $feed_i$ is the sensory feedback signal which is necessary for stable bipedal walking. τ and τ' are time constants which have influence on the shape and period of the output signal. n is the number of neural oscillators.

A biological rhythmic locomotion is performed by the sequence of extension and flexion of muscles. When one side of the body part is extending, the other side is flexing, and the extension and flexion continue alternately. For the modeling of this biological system, in this paper, the CPG structure proposed by Taga [19] is employed to generate the COM height trajectory. In this structure, the basic rhythmic locomotion is assumed to be generated by the neural oscillators, each of which consists of two mutually excited neurons: an extensor neuron and a flexor neuron. They are closely interconnected in the same neural oscillator and alternately generate the flexion and extension signals. By the effect of this relationship, the rhythmic signals are generated.

B. COM Height Trajectory Generation Using CPG

The COM height trajectory is generated by the CPG as follows:

$$z = Z_c + z_{cpg} \tag{8}$$

with

$$z_{cpg} = A_z(y_1 - y_2 - 1)$$

where A_z is the amplitude scaling factor, z_{cpg} is generated by the CPG for the COM height variation and y_1 and y_2 perform the extensor and flexor neuron roles, respectively. To compensate the disturbance caused by the COM height variation, the sensory feedback is designed, which guarantees the stability while walking. It is defined by the GRFs on the feet while walking, which are measured by four force sensing resisters (FSRs) equipped on the sole of each foot, as follows:

$$\begin{aligned} feed_1 &= k_f |F_l + F_r - mg| \\ feed_2 &= -feed_1 \end{aligned} \tag{9}$$

where k_f is the scaling factor and F_l and F_r are the GRFs on the left and right feet, respectively.

C. Evolutionary Optimization for CPG

This section presents evolutionary optimization for the CPG. In this paper, the QEA [26], [27] is employed to optimize the CPG.

1) Quantum-inspired Evolutionary Algorithm (QEA): To explore the search space of optimization problems effectively, the QEA was proposed using the concept of quantum computing. The QEA starts with a global search and changes automatically into a local search as the generation advances because of its inherent probabilistic mechanism. Thus, it leads to a good balance between exploration and exploitation. Moreover, the QEA utilizes subpopulations and shares information among them using global and local migration operations for a parallel structure.

2) Optimization: Firstly, the period of the trajectory generated by the evolutionary optimized CPG should be equal to the walking period $T^{ss}_{l/r} + T^{ds}_{l/r}$. Moreover, the amplitude of the trajectory at every period should be equal to each other and the difference between the amplitude and A_z should be minimized. In addition, the GRFs on the feet while walking should be minimized. To satisfy these conditions, u_0, τ, and τ' in the neural oscillator and k_f in the sensory feedback are obtained by the QEA and the objective function is defined as follows:

$$f = k_p f_p + k_d f_d + k_a f_a + k_g f_g + P \tag{10}$$

with

$$\begin{aligned} f_p &= |T_{cpg} - (T^{ss}_{l/r} + T^{ds}_{l/r})| \\ f_d &= |A^f_{cpg} - A^i_{cpg}| \\ f_a &= |A_z - A^f_{cpg}| \\ f_g &= \sum |F_l + F_r - mg| \end{aligned}$$

where k_p, k_d, k_a, and k_g are the scaling factors, T_{cpg} is the period of the trajectory generated by the evolutionary optimized CPG, and A^i_{cpg} and A^f_{cpg} are the amplitudes at the initial and final periods of the trajectory, respectively. P is the penalty value which is given when the robot falls down while walking.

IV. SIMULATIONS

The proposed method is applied to the simulation model of the small-sized bipedal robot, HSR-IX (Fig. 2) modeled by Webot which is the 3-D robotics simulation software and enables users to conduct the physical and dynamical

simulation [28]. HSR has been in continual development and research by the Robot Intelligence Technology laboratory, KAIST [11]. Its height and weight are 52.8 cm and 5.5 kg, respectively. It has 26 DOFs which consist of 12 DC motors with harmonic drives in the lower body and 16 RC servo motors in the upper body (two servo motors in each hand control). The on-board Pentium-III compatible PC, running RT-Linux, calculates the proposed algorithm every 5 msec in real-time. To measure the GRFs on the feet and the real ZMP trajectory while walking, four FSRs are equipped on the sole of each foot.

A. Evolutionary Optimized CPG by QEA

In the simulations, Z_c was set as 25.2 cm. The parameters in the CPG, u_1, u_2, v_1, and v_2 were set as 0.695, 0.098, 0.283, and 0.521, respectively to make initial value of z_{cpg} to zero. w_{12} and w_{21} were set as 1.5 and 1.5, respectively to make the phase difference between y_1 and y_2 to π and β was set as 2.5 [20]. k_p, k_d, k_a, and k_g were taken as 20.0, 1.0, 1.0, and 0.0002, respectively and P was set as $+\infty$. $T_{l/r}^{ss}$ and $T_{l/r}^{ds}$ were set as 0.8 s and 0.4 s, respectively and A_z was set as 1.0. u_0, τ, τ', and k_f optimized by the QEA were obtained as 2.1301, 0.1411, 0.4826, and -0.001987, respectively. Consequently, T_{cpg}, A_{cpg}^{i}, and A_{cpg}^{f} were obtained as 1.2 s, 1.0 cm, and 1.0 cm, respectively.

B. Walking Simulation Results

Fig. 3 shows the snapshots of the simulation result of straight walking using the COM height trajectory generated by the evolutionary optimized CPG. As the figure shows, the robot walked stably with the variable COM height like humans. Fig. 4 shows the COM height trajectories generated by the evolutionary optimized CPG and the sinusoidal function utilized in [18]. The thick and thin lines represent the COM trajectories in the single and double support phases, respectively. In the simulation, the maximum stride length was 9.8 cm when the robot walked with the COM height trajectory generated by the evolutionary optimized CPG. It was larger than the maximum stride lengths, 7.5 cm and 8.0 cm, when the robot walked with the constant COM height and the COM height trajectory generated by the sinusoidal function, respectively. It was because the robot could avoid the singularities by the lower COM height in the double support phase.

Fig. 5 shows the measured ZMP trajectories while walking using the COM height trajectory generated by the evolutionary optimized CPG. As shown in the figure, the ZMP trajectories in x-axis and y-axis followed the foot trajectories with a small variation. The small variation of the ZMP trajectories was mainly caused by the COM height variation and the dynamic difference between the robot and the 3-D LIPM. However, by the evolutionary optimized sensory feedback signals in the CPG as shown in Fig. 6, the GRFs on the feet while walking were minimized as shown in Fig. 7. Thus, the variation of the ZMP trajectories was minimized. Consequently, the ZMP trajectories were within the upper and lower boundaries of foot trajectories. Also, as shown in Fig. 8, the robot was able to modify walking patterns while walking stably using the COM height trajectory generated by the evolutionary optimized CPG. Table I shows the CS list used for this simulation, in which sagittal and lateral step lengths and direction of the swing leg were independently changed while maintaining the same walking period at each footstep.

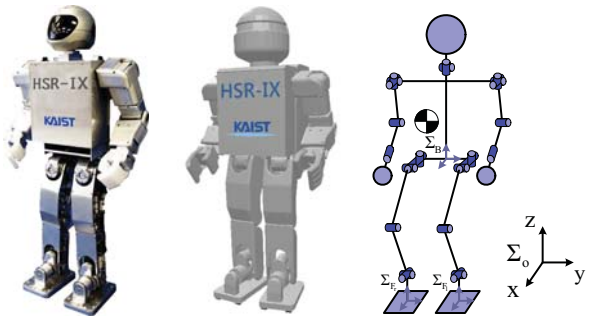

(a) (b) (c)

Fig. 2. (a) HSR-IX. (b) Simulation model. (c) Configuration.

V. CONCLUSION

In this paper, the human-like bipedal walking with a large stride by the height variation of the COM using an evolutionary optimized CPG was proposed. The walking pattern for the bipedal robot was generated by the MWPG and the COM height trajectory was generated by the CPG. The CPG with the sensory feedback was optimized by the QEA. The proposed method was verified through the simulations for the simulation model of the small-sized bipedal robot, HSR-IX. Consequently, the bipedal robot could walk stably like humans with modifiable walking patterns and a large stride by the height variation of the COM using the evolutionary optimized CPG.

VI. ACKNOWLEDGMENTS

This research was supported by Basic Science Research Program through the National Research Foundation of Korea (NRF) funded by the Ministry of Education, Science and Technology (2011-0000321).

REFERENCES

[1] Y. Sakagami, R. Watanabe, C. Aoyama, S. Matsunaga, N. Higaki, and K. Fujimura, "The intelligent ASIMO: system overview and integration," in *Proc. IEEE/RSJ Int. Conf. Intell. Robot. Syst.*, 2002, vol. 3, pp. 2478–2483.

[2] K. Akachi, K. Kaneko, N. Kanehira, S. Ota, G. Miyamori, M. Hirata, S. Kajita, and F. Kanehiro, "Development of humanoid robot HRP-3P," in *Proc. IEEE-RAS Int. Conf. Humanoid Robots*, 2005, pp. 50–55.

[3] Y. Ogura, H. Aikawa, K. Shimomura, H. Kondo, A. Morishima, H.-O. Lim, and A. Takanishi, "Development of a new humanoid robot WABIAN-2," in *Proc. IEEE Int. Conf. Robot. Autom.*, 2006, pp. 76–81.

[4] S. Kajita, F. Kanehiro, K. Kaneko, K. Fujiwara, K. Yokoi, and H. Hirukawa, "A realtime pattern generator for biped walking," in *Proc. IEEE Int. Conf. Robot. Autom.*, 2002, vol. 1, pp. 31–37.

[5] N. Motoi, T. Suzuki, and K. Ohnishi, "A bipedal locomotion planning based on virtual linear inverted pendulum mode," *IEEE Trans. Ind. Electron.*, vol. 56, no. 1, pp. 54–61, Jan. 2009.

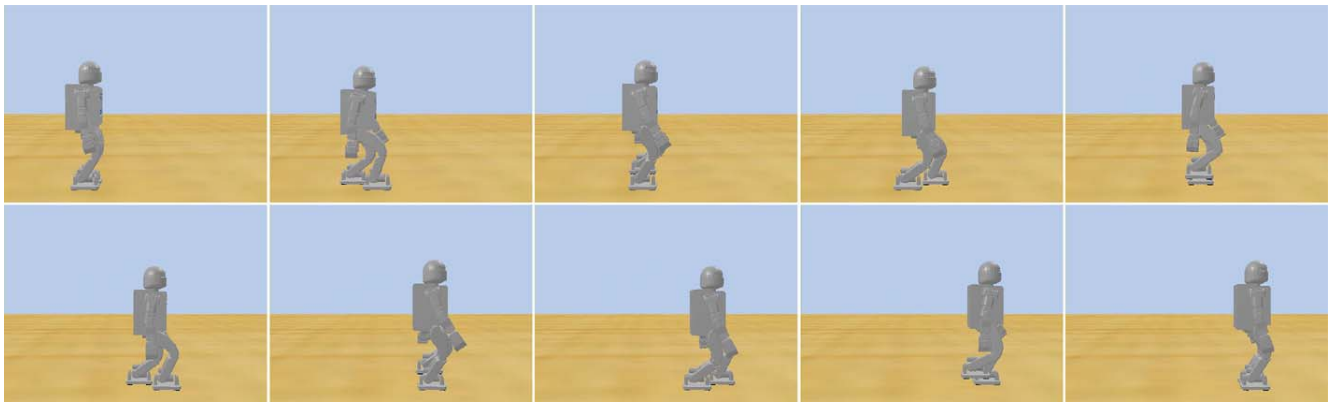

Fig. 3. Snapshots of the simulation result of straight walking using the COM height trajectory generated by the evolutionary optimized CPG (left to right, top to bottom).

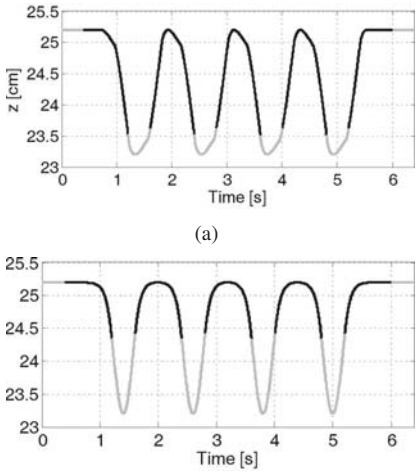

Fig. 4. COM height trajectory generated by (a) the evolutionary optimized CPG and (b) the sinusoidal function. The thick and thin lines represent the COM trajectories in the single and double support phases, respectively.

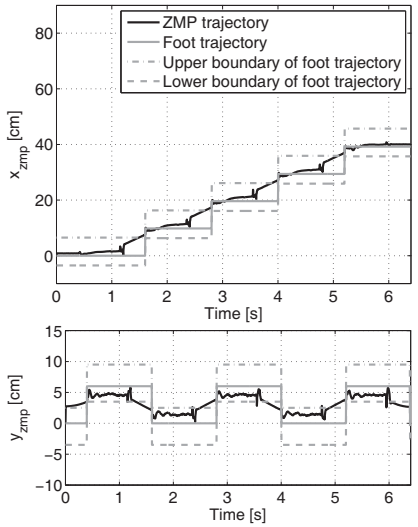

Fig. 5. Measured ZMP trajectories while walking using the COM height trajectory generated by the evolutionary optimized CPG.

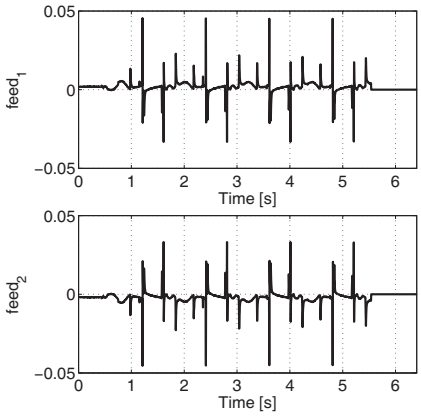

Fig. 6. Evolutionary optimized sensory feedback signals in the CPG.

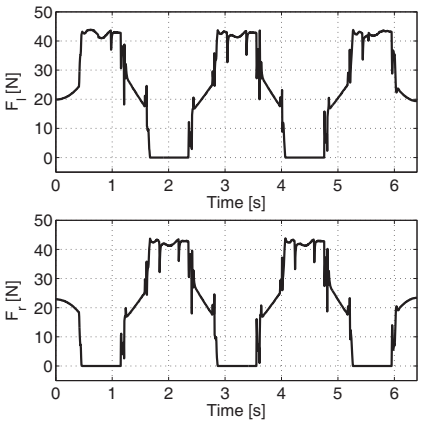

Fig. 7. Left and right GRFs while walking using the COM height trajectory generated by the evolutionary optimized CPG.

[6] K. Erbatur and O. Kurt, "Natural ZMP trajectories for biped robot reference generation," *IEEE Trans. Ind. Electron.*, vol. 56, no. 3, pp. 835–845, Mar. 2009.

[7] T. Sato, S. Sakaino, and K. Ohnishi, "Real-time walking trajectory generation method with three-mass models at constant body height for three-dimensional bipedal robots," *IEEE Trans. Ind. Electron.*, vol. 58, no. 2, pp. 376–383, Feb. 2011.

[8] S. Kajita, F. Kanehiro, K. Kaneko, K. Fujiwara, K. Harada, K. Yokoi, and H. Hirukawa, "Biped walking pattern generation by using preview control of zero-moment point," in *Proc. IEEE Int. Conf. Robot. Autom.*,

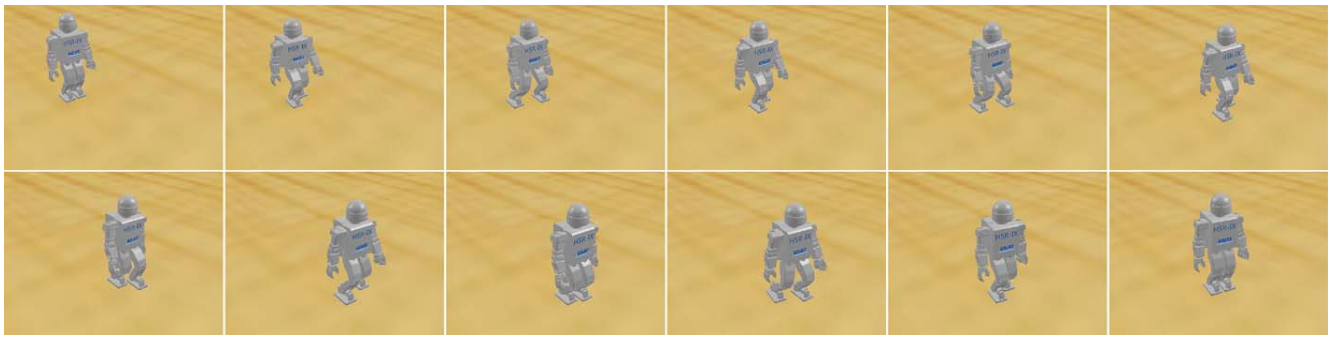

Fig. 8. Snapshots of the simulation result of modification of walking patterns while walking using the COM height trajectory generated by the evolutionary optimized CPG (left to right, top to bottom).

TABLE I

CS LIST (TIME UNITS, LENGTH UNITS, AND ANGLE UNITS WERE GIVEN IN SECONDS, CENTIMETERS AND DEGREES, RESPECTIVELY.)

Steps	T_l^{ss}	T_l^{ds}	S_l	L_l	θ_l	T_r^{ss}	T_r^{ds}	S_r	L_r	θ_r
1^{st}	0.8	0.4	7.0	6.0	0.0	0.8	0.4	7.0	-6.0	0.0
2^{nd}	0.8	0.4	4.0	13.0	0.0	0.8	0.4	4.0	-6.0	0.0
3^{rd}	0.8	0.4	7.0	6.0	0.0	0.8	0.4	7.0	-6.0	0.0
4^{th}	0.8	0.4	4.0	13.0	0.0	0.8	0.4	4.0	-6.0	0.0
5^{th}	0.8	0.4	9.0	6.0	0.0	0.8	0.4	9.0	-8.0	0.0
6^{th}	0.8	0.4	7.0	6.0	0.0	0.8	0.4	7.0	-6.0	0.0
7^{th}	0.8	0.4	5.0	6.0	0.0	0.8	0.4	5.0	-11.0	0.0
8^{th}	0.8	0.4	2.0	6.0	0.0	0.8	0.4	2.0	-6.0	0.0
9^{th}	0.8	0.4	-6.0	6.0	0.0	0.8	0.4	-6.0	-9.0	-10.0
10^{th}	0.8	0.4	-6.0	6.0	0.0	0.8	0.4	-6.0	-6.0	0.0
11^{th}	0.8	0.4	0.0	6.0	0.0	0.8	0.4	0.0	-6.0	0.0

2003, vol. 2, pp. 1620–1626.

[9] K. Harada, S. Kajita, K. Kaneko, and H. Hirukawa, "An analytical method on real-time gait planning for a humanoid robot," in *Proc. IEEE-RAS Int. Conf. Humanoid Robots*, 2004, vol.2, pp. 640–655.

[10] B.-J. Lee, D. Stonier, Y.-D. Kim, J.-K. Yoo, and J.-H. Kim, "Modifiable walking pattern of a humanoid robot by using allowable ZMP variation," *IEEE Trans. Robot.*, vol. 24, no. 4, pp. 917–925, Aug. 2008.

[11] Y.-D. Hong, B.-J. Lee, and J.-H. Kim, "Command state-based modifiable walking pattern generation on an inclined plane in pitch and roll directions for humanoid robots," *IEEE/ASME Trans. Mechatron.*, vol. 16, no. 4, pp. 783–789, Aug. 2011.

[12] R. Kurazume, S. Tanaka, M. Yamashita, T. Hasegawa, and K. Yoneda, "Straight legged walking of a biped robot," in *Proc. IEEE/RSJ Int. Conf. Intell. Robot. Syst.*, 2005, pp. 337–343.

[13] M. Morisawa, S. Kajita, K. Kaneko, K. Harada, F. Kanehiro, K. Fujiwara, and H. Hirukawa, "Pattern generation of biped walking constrained on parametric surface," in *Proc. IEEE Int. Conf. Robot. Autom.*, 2005, pp. 2405–2410.

[14] A. Sekiguchi, K. Kameta, Y. Tsumaki, and D. N. Nenchev, "Biped walk based on vertical pivot motion of linear inverted pendulum," in *Proc. IEEE/ASME Adv. Intell. Mechatron.*, 2007, pp. 1–6.

[15] K. Terada and Y. Kuniyoshi, "Online gait planning with dynamical 3D-symmetrization method," in *Proc. IEEE-RAS Int. Conf. Humanoid Robots*, 2007, pp. 222–227.

[16] S. Shimmyo, T. Sato, and K. Ohnishi, "Biped walking pattern generation by using preview control with virtual plane method," in *Proc. IEEE Int. Work. Adv. Motion Control*, 2010, pp. 414–419.

[17] S. Shimmyo and K. Ohnishi, "Nested preview control by utilizing virtual plane for biped walking pattern generation including COG up-down motion," in *Proc. IEEE Annu. Conf. Ind. Electron. Soc.*, 2010, pp. 1571–1576.

[18] Z. Li, B. Vanderborght, N. G. Tsagarakis, and D. G. Caldwell, "Fast bipedal walk using large strides by modulating hip posture and toe-heel motion," in *Proc. IEEE Int. Conf. Robot. Biomimetics*, 2010, pp. 13–18.

[19] G. Taga, "A model of the neuro-musculo-skeletal system for human locomotion," *Biol. Cybern.*, vol. 73, pp.97–111, 1995.

[20] K. Matsuoka,"Mechanisms of frequency and pattern control in the neural rhythm generators," *Biol. Cybern.*, vol. 56, no. 5, pp. 345–353, Jul. 1987.

[21] G. Endo, J. Nakanishi, J. Morimoto, and G. Cheng, "Experimental studies of a neural oscillator for biped locomotion with QRIO," in *Proc. IEEE Int. Conf. Robot. Autom.*, 2005, pp. 596–602.

[22] L. Righetti and A. J. Ijspeert, "Programmable central pattern generators: an application to biped locomotion control," in *Proc. IEEE Int. Conf. Robot. Autom.*, 2006, pp. 1585–1590.

[23] K. Watanabe, G. L. Liu, M. K. Habib, and K. Izumi, "Neural oscillators with a sigmoidal function for the CPG of biped robot walking," in *Proc. IEEE Annu. Conf. Ind. Electron. Soc.*, 2007, pp. 128–133.

[24] M. K. Habib, K. Watanabe, and K. Izumi, "Biped locomotion using CPG with sensory interaction," in *Proc. IEEE Int. Symp. Ind. Electron.*, 2009, pp. 1452–1457.

[25] C.-S. Park, Y.-D. Hong, and J.-H. Kim, "Full-body joint trajectory generation using an evolutionary central pattern generator for stable bipedal walking," in *Proc. IEEE/RSJ Int. Conf. Intell. Robot. Syst.*, 2010, pp. 160–165.

[26] K.-H. Han and J.-H. Kim, "Quantum-inspired evolutionary algorithm for a class of combinatorial optimization," *IEEE Trans. Evol. Comput.*, vol. 6, no. 6, pp. 580–593, Dec. 2002.

[27] K.-H. Han and J.-H. Kim, "Quantum-inspired evolutionary algorithms with a new termination criterion, Hϵ gate, and two phase scheme," *IEEE Trans. Evol. Comput.*, vol. 8, no. 2, pp. 156–169, Apr. 2004.

[28] O. Michel, "Cyberbotics Ltd. WebotsTM: Professional mobile robot simulation," *Int. J. Adv. Robot. Syst.*, vol. 1, no. 1, pp. 39–42, 2004.